UNIVERSITY OF CALIFORNIA
SANTA CRUZ

# AUTOMATED TOOLS FOR ACCURATE AND PRECISE DOSING OF GRANULAR SOLIDS

A thesis submitted in partial satisfaction of the
requirements for the degree of

BACHELOR'S OF SCIENCE

in

ROBOTICS ENGINEERING

by

**John R. Minnick**

November 2023

# Table of Contents

# List of Figures

# List of Tables

## Abstract

Automated Tools for Accurate and Precise Dosing of Granular Solids

by

John R. Minnick

The process of automated powder dosing is investigated. Common pitfalls in powder dosing technologies are acknowledged. Conveyance and feedback methods are reviewed. The necessity of a closed loop system for accurate powder dosing is demonstrated. A prototype of a pumping element is introduced. The pumping element and load cell are subjected to testing. The tests show that the pumping element and load cell achieve decigram accuracy with a margin of safety of 6. Future revisions to the pumping element, load cell, and control flow are proposed. It is theorized with these revisions that long term milligram accuracy can be achieved.

To my parents, peers, and professors

without their love, support, and guidance

I would have never made it past freshman year.

## Acknowledgments

There are a great many people who I would like to thank for their contributions to my thesis and my academic career. I would like to thank my PI, Mircea, who gave me the opportunity to work, learn, and fail in his lab. I would like to thank my academic advisor, Monique Vairo, who was always there to guide me when I lost my way. I would like to thank Yohei Rosen for his endless patience when working with me and his guidance on matters I was unfamiliar with. I would like to thank Kivilcim Doganyigit for being a good friend and role model, especially when I made it very hard to be my friend. I would like to thank Gordon Keller, for taking me under his wing (or possibly under his rotor) when I first joined the lab. I want to thank, in no particular order: Drew Ehrlich, Nico Hawthorne, Ash Robbins, Maryam Tebyani, Kateryna Voitiuk, Pierre Baudin, and Sebastián Torres Montoya. These people were kind to me, helped me to learn and grow, and were overall good role models and good people to be around.

One last time, I would like to thank everyone who has helped me along the way, both those named here and the unmentioned nameless. I would not have been able to do this alone. Because of you, the trajectory of my life has been changed for the better. With every cubic inch of my heart, I thank you.

# Chapter 1

# Introduction

Automated accurate and precise dosing of granular solids is a required task in many fields of science and engineering. The majority of affordable commercially available devices are poorly designed and carelessly made. A large amount of these devices operate blindly, with no feedback loop. Even more of these devices are constructed out of plastic. Using plastic is great for production, but leads to devices that lack precision. Plastic parts also wear over time due to abrasion from the granular flow. The few automated devices which maintain their accuracy and precision overtime are exuberantly expensive.

It is believed that an automated closed-loop system that can dose granular solids with decigram[1] accuracy is achievable. Furthermore, it is believed that such a system can be manufactured to withstand the test of time. In order to achieve this, two primary elements must be composed and brought together harmoniously. First and

[1] Or even milligram!

foremost, a feedback system is necessary due to the unpredictable nature of powder flow. The system must be closed loop. Secondly, a precision pumping element capable of making micro-adjustments to the dosage is needed. Acquiring milligram accurate feedback is useless if we cannot act upon it. These to two primary elements were investigated and the results reported in this thesis document.

# Chapter 2

# Objective

An affordable robotic system capable of safely storing and accurately dosing corrosive powders over long periods of time is desired.

Specifications for such a system are:

- The system must be able to repeatedly dispense a constant mass of powder with variations of less than one (1) decigram. To this end, the bigger the margin of safety the better and the objective will be not to hit decigram accuracy but instead to surpass it.

- The system must be able to maintain its calibration and function with negligible drifting over the course of at least three (3) months.

- The system cannot be exorbitantly overprice, as this would make the machine inaccessible to possible users which lack significant funds. To be brief, the system should cost less than 1000 USD and preferably less than 500 USD.

- The system must be constructed out of non-reactive materials so as to not contaminate the environment it is intended for. Materials allowed for construction are non-reactive plastics and three hundred and sixteen (316) grade stainless steel or higher.
- The system must be able to function over the course of at least (3) months without human intervention.

# Chapter 3

# Literature Review

Let us now consider the common[1] ways of both conveying and measuring granular solids. The review conducted here will hopefully help us to make wise design choices and avoid common pitfalls.

## 3.1 Methods of Conveyance

### 3.1.1 Pneumatic Conveyance

Pneumatic conveyors move powder by creating pressure differentials between two or more points. Pneumatic systems are high throughput and handle powders without crushing or compacting them. They are ideal for handling large amounts of hazardous or hydrophilic powder across short distances. The downside is that pneumatic systems are expensive to build and maintain. They require pressure seals, air filters, vents, and significant maintenance. Additionally, pneumatic systems require complex

[1] And uncommon.

controllers to keep everything running smoothly.

### 3.1.2 Belt Conveyor

Belt conveying, similar to pneumatic conveying, can handle large volumes of bulk powder across short distances. The difference between these methods is that belt conveyors require significantly less financial investment and maintenance. However, if the powder being handled is hazardous or hydrophilic, it would be unwise to use an open air belt conveyance system. Belt conveyance is better suited for industrial mining operations which need to transport bulk loose solids.

### 3.1.3 Bucket Conveyor

Bucket conveying is one of the most gentle methods powder handling available [11]. It avoids crushing or compacting the powder being handled. Bucket conveying also is able to have high throughput. An attractive quality of bucket conveying for powder dosing is that powder is handled in discrete batches of roughly the same quantity. The weakness of this method is that under normal atmospheric conditions each batch of powder will significantly vary from every other batch. This is due to density variations across each batch, also known as force chains[2]. It would be unwise to attempt a theoretical analysis of bucket discharge [14].

[2]Force chains are the chains of compressive forces that occur across granular particles. Think about breaking a triangle of billiards balls at the start of a game of billiards. Some of the balls go flying about the table, while others may not move at all. This is an example of the propagation of force chains

### 3.1.4 Vibration Aided Gravitational Conveyance

Vibration aided gravitational conveyance is an effective method with several critical caveats that must be considered. It has been shown that powders will fluidize when vibrated at specific frequencies [23]. Fluidization of a powder decreases density variations across a powder by breaking down the force chains that propagate within the bulk powder. Breaking apart the force chains which naturally occur in bulk solids is advantageous for many reasons. It allows for continuous closed loop dispensation through feedback of a flow sensor. Additionally, if uniformity of powder across some volume is desired, fluidization is one of the most effective, low cost options available. In short, there are less factors to consider in fluids dynamics than in powder dynamics. Thus, fluidizing a powder will typically lower the computational complexity of metering it.

Fluidizing a powder with vibrations comes with some major trade-offs. A large portion of the sensing technology for detecting density variations within a powder are susceptible to vibrational noise. A prime example of this is the sensing technology of acoustic emission. Acoustic emission is an effective, low cost method of sensing density variations [5]. However the acoustic noise generated by vibrational fluidization significantly lowers the signal-to-noise (SNR) ratio. This phenomena is present across other sensing technologies as well, with acoustic emission being the most susceptible. If one wishes to pair a vibrational conveyance method with an sensing method susceptible to vibrational noise, it would be wise to strongly isolate the two from each other.

### 3.1.5 Classical Archimedes Screw

Screw conveyance is one of the oldest and most popular methods for bulk powder conveyance. Screw conveyors are simple, clean, and efficient when it comes to handling free flowing powders. However, "the mechanics of the conveying action is very complex and designers tend to rely heavily on empirical performance data."[15]

A screw conveyor provides the amount of control desired for precision applications. This control cannot be realized in an open loop system. In order to make effective use of this control, an equally precise sensor feedback method would need to be implemented in order to close the control loop.

The classical Archimedes screw also suffers from feeding issues. In the classical Archimedes setup, the threads of the screw are exposed and these exposed thread make up the inlet. These exposed threads suffer from significant feeding issues. By allowing the bulk solid to naturally feed itself into the screw, large density variations can and do occur.

### 3.1.6 Old's Elevator

The working principle of an Old's Elevator is similar to that of a classical Archimedes screw with a slight relativistic twist. Instead of the screw rotating within a housing to induce upwards flow as in a classical screw elevator setup, an Old's Elevator has the housing rotate about the screw. The Old's Elevator provides several significant advantages over the classical Archimedes screw [13].

The Old's Elevator generates less dust while working. This is ideal when

handling chemically hazardous or flammable powders. The Old's Elevator provides a more stable flow rate than a traditional screw. The flow rate of an Old's Elevator has a strong linear correlation to the rotational speed of the housing. This allows for better dosage accuracy and precision in an open-loop system and better control in a closed-loop system. It has been shown that the Old's Elevator also causes less segregation and clumping that a classical screw elevator.

## 3.2 Methods of Feedback

### 3.2.1 Near Infrared Imaging

As seen in [18], near infrared imaging can be used to implement both a feed-forward and feed-back control system. This method is fast and contactless way to measure the density of a volume of powder. If the volume of the powder is constant and the density sensor data is accurate, then the mass of the powder can be determined.

There are two major drawbacks of near infrared imaging. The first is the limited penetration depth of near infrared imaging systems. The powder sample would need to be kept exceedingly thin in order to achieve near infrared penetration. Secondly, the data gathered from near infrared imaging would be meaningless without an accurate empirical model to map it to. It would take time and specialized equipment to build such a model.

### 3.2.2 Microwave Imaging

Microwave imaging can be used as a feedback method for powder density. Microwaving imaging allows for rapid and contactless measurement. The drawback of this method is that the microwave imaging resolution increases as the imaging media becomes more hydrated [22]. This method would not work well with dry powders. This method also suffers from the need for an accurate empirical model; however most of the sensor systems mentioned in this document suffer from the same problem.

### 3.2.3 Electrical Capacitance Tomography

Electrical capacitance tomography can be used to acquire meaningful data about the cross-section of the powder sample being observed. This method is contactless and can preform rapid cross section imaging of a flowing powder[24].

The drawback of this method is the underlying complexity that must be achieved to receive meaningful sensor feedback. The process is computationally intensive. The process also requires that the mass flow rate of the powder past the sensor to remain relatively constant. This is easily achievable for a fluid, and much less achievable for a powder.

### 3.2.4 Ultrasonic Sensing

Ultrasonic sensing can be used to obtain accurate density measurements in a powder[20]. Ultrasonic sensing requires minimal calibration and is a contactless method. However, ultrasonic sensors are highly vulnerable to external noise corrupting the signal

integrity.

### 3.2.5 Acoustic Emission

Acoustic emission can be used for measuring powder density [5]. However, it faces the same problems as ultrasonic sensing. It is highly vulnerable to external noise corrupting the signal integrity. This may not be suited for an environment where other machines are operating.

### 3.2.6 Strain Gauge

A strain gauge is the classical method to determine the amount of force being applied to an object. Strain gauges are well suited for the task of automatically dosing powder [10]. A suitable model is required in order to make accurate measurements with a strain gauge. Additionally, a strain gauge should be allowed a certain amount of settling time before measurements can be taken [9]. While strain gauges are capable of providing continuous flow rate feedback; the necessary models to do so are much more complex than the ones needed for preforming discrete measurements.

## 3.3 Design Choices

From the literature review, the decision was made implement a strain gauge as an accurate and cost effective method of acquiring feedback. As for the pumping element, it was decided that an Old's Elevator would be wise to pursue. The data [13] indicates that an Old's Elevator has better flow properties than a conventional screw.

# Chapter 4

# Materials and Methods

## 4.1 Materials

The materials used in both the manufacturing of the system as well as the testing of said system in no particular order are as follows:

- Prusa MK3S 3D Printer
- PETG 3D Printing Filament
- Sandpaper (ranging from 80 grit to 320 grit)
- 316 Stainless Steel Sheet Metal
- Varied 316 Stainless Steel Fasteners
- HX711 Load Cell Driver Board
- 500 Gram Rated Load Cell
- ROB-12779 Stepper Motor Driver Board
- CF-31 Toughbook Laptop
- Analog Discovery 2
- Laboratory Grade Calibration Weights
- Torque Wrench and Torque Screwdriver

- Laboratory Balance (+/- 0.001 gram accuracy)
- Laboratory Grade Sodium Bicarbonate Powder
- Manual Lathe
- CNC Mill
- Drill Press
- Bench Grinder
- Polishing Wheel

## 4.2 Methods

The methodology for running pump tests and gathering pump data was to implement loss-in-weight techniques in conjunction with the apparatus seen in 5.6 and a laboratory grade balance. Data analyzation techniques where drawn from [3] and [2], who's previous work in this area formed the fundamental basis for this thesis. Further detail regarding pumping element tests will be discussed in a later section of this thesis.

The methodology for conducting load cell test was to implement extremely accurate (+/- 0.001 gram) known weights to build a highly accurate model in order to map load cell output to true weight. Further detail regarding load cell tests will be discussed in a later section of this thesis.

# Chapter 5

# Design and Results

## 5.1 Characterization of Sodium Bicarbonate Powder

Sodium bicarbonate ($NaHCO_3$) powder is a common material used in industrial manufacturing. The characteristics of sodium bicarbonate powder were investigated using various tests. This was done to build a better understanding of the flow properties of sodium bicarbonate powder and to avoid unwise design choices.

### 5.1.1 Bulk Density Test

The bulk density of sodium bicarbonate powder was needed to make design choices regarding the size of the bulk storage tank and powder pump. The bulk density of a powder defined as the mass of the powder divided by its volume. A laboratory grade graduated cylinder was used to measure the volume of sodium bicarbonate powder. A laboratory grade scale was used to measure the mass of sodium bicarbonate powder.

The bulk density was calculated using equation 5.1.

$$\rho_b = \frac{m}{V} \tag{5.1}$$

where $\rho_b$ is the bulk density, $m$ is the mass of the powder, and $V$ is the volume of the container.

The bulk density of the sodium bicarbonate powder used throughout this project was measured and found to be 0.88 g/cm$^3$ at 21 degrees Celsius.

### 5.1.2 Angle of Repose Test

The angle of repose of sodium bicarbonate was needed to make design choices regarding the feed funnel to the powder pump. The angle of repose of a powder is the maximum angle that the surface of the powder can make with a horizontal plane before the powder begins to flow [1]. Knowing this angle is crucial to keep the pump inlet saturated. The angle of repose of sodium bicarbonate powder was measured by slowly pouring the powder through a funnel onto a flat surface. The angle of repose was calculated using the equation 5.2.

$$\theta = \tan^{-1}\left(\frac{h}{r}\right) \tag{5.2}$$

where $\theta$ is the angle of repose, $h$ is the height of the cone, and $r$ is the radius of the base of the cone.

The measured angle of repose of the sodium bicarbonate powder was 28 degrees. In order to ensure that the powder pump inlet remains saturated, the feed angle

of the funnel should be greater than 28 degrees from its horizontal plane.

## 5.2 Weight Feedback System

### 5.2.1 Low-End Weight Feedback System Design

The ADC selection was primarily determined by the required resolution and sampling rate. The required bit resolution ($N$) of the ADC is related to the minimum force you want to measure ($F_{\text{min}}$) and the operating range ($F_{\text{max}}$) of the load cell 5.3.

$$N = \log_2\left(\frac{F_{\text{max}}}{F_{\text{min}}}\right) \tag{5.3}$$

In our application, ($F_{\text{min}}$) is 0.10 grams and ($F_{\text{max}}$) is 500 grams.

$$N = \log_2\left(\frac{500}{0.10}\right) \tag{5.4}$$

Thus, N equates to:

$$N = 12.2877 \tag{5.5}$$

Meaning that in order to achieve decigram resolution, the selected ADC needs to have a bit count of 13 or higher. In application, a 24-bit $\Sigma\Delta$ ADC was chosen. This means that the theoretical $F_{\text{min}}$ equates to 0.00003 grams. However, in practice this is not realistic as real signals contain noise, and thus a certain amount of the bits are lost to this noise. Later on we will see that the weight feedback system can achieve a

resolution of about 0.015 grams experimentally. This correlates to 15 effective bits out of the 24.

$$t_s = 5seconds \tag{5.6}$$

In our specific application, as long as enough settling time is allowed to pass, the signal was found to be static. From 5.4 and 5.5, we can see a maximum settling time of 5 seconds. Thus by heavily oversampling our signal at a rate of 10 times per second after allowing it to settle, we are able to achieve stable output from the ADC with negligible variation.

### 5.2.2 Low-End Weight Feedback System Tests

The low-end weight feedback system was experimentally tested. A 500 gram rated 4-wire load cell and a HX711 24-bit analog-to-digital converter were used as the subject for experiment. A set of laboratory grade calibration weights rated to one-tenth of a milligram accuracy were used as the control weights for this experiment. Tests results 5.3 5.4 5.5 indicate that the low-end weight feedback system can accurately track weights within the 0 gram to 100 gram range with a maximum error of 2 centigrams occurring at the ends of the linear region. Test results 5.3 5.4 5.5 also indicate that the low-end weight feedback system can precisely track weights with a variance of 15 milligrams between independent readings.

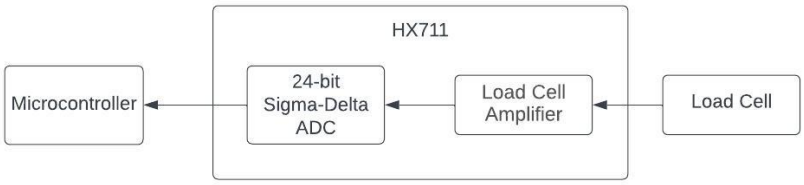


Figure 5.1: Block Diagram of Low-End Weight Feedback System

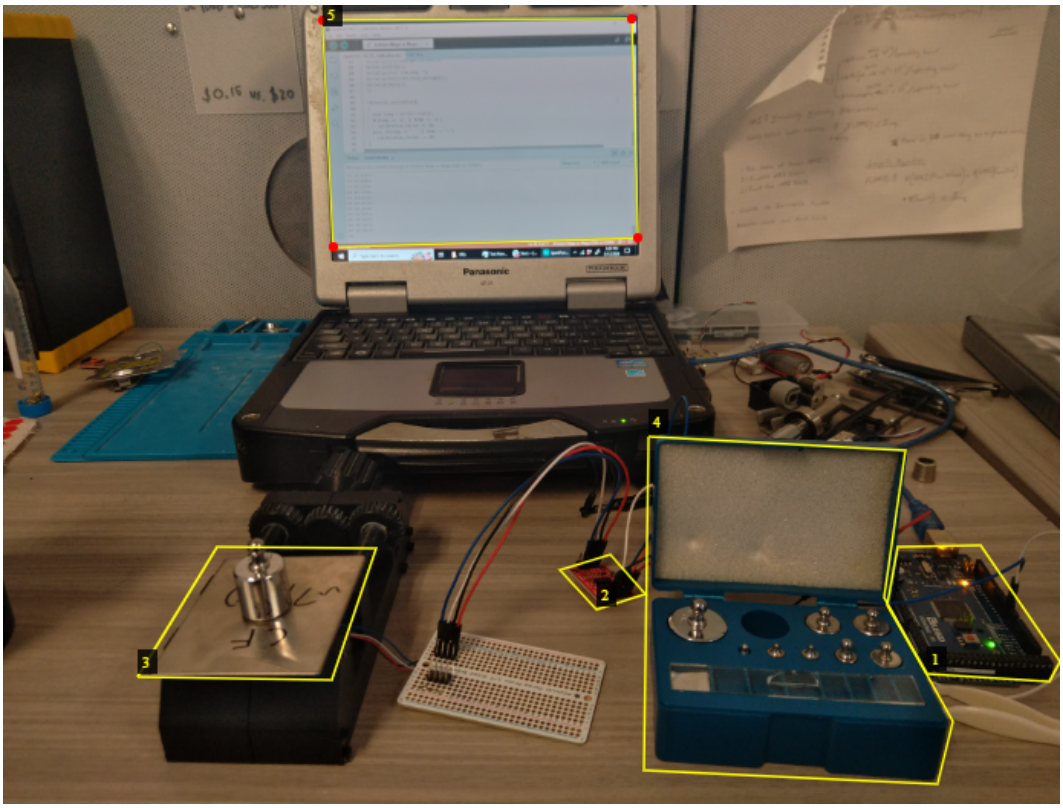


Figure 5.2: Setup of the Low-End Weight Feedback System. (1) The micro-controller. (2) HX711 Amplifier & $\Sigma\Delta$ ADC. (3) The load cell being validated with a 50 gram calibration mass. (4) The set of masses used for calibrating this system. (5) The terminal used for acquisition and validation of load cell data .

The load cell was securely mounted to the workbench by way of steel mounting

bolts. Mounting bolts were installed using a torque wrench. The matching torques of the mounting bolts ensures that strain induced by the load is uniformly dispersed across the cell. A linearized equation converting the ADC reading to a weight was determined using a 3-point calibration method. The equation was intentionally designed to operate within the 0 to 100 gram range. Outside of this range, the accuracy begins to step outside of a decigram5.5. The load cell, HX711, and conversion equation were evaluated for both accuracy and precision.

The accuracy test consisted of applying the calibration weights to the load cell and comparing the resulting output to the true value. This allows us to quantify how accurate our weight measurements are as well as the effective range in which we can accurately measure a weight before stepping out of the linear region of our conversion equation.

The precision test consisted of repeating the accuracy tests in triplicate. The resulting outputs from each set of accuracy tests was recorded and compared to each other. This allows for us to quantify how precise our weight measurements are as well as the effective range in which we can precisely measure a weight before stepping out of the linear region of the conversion equation.

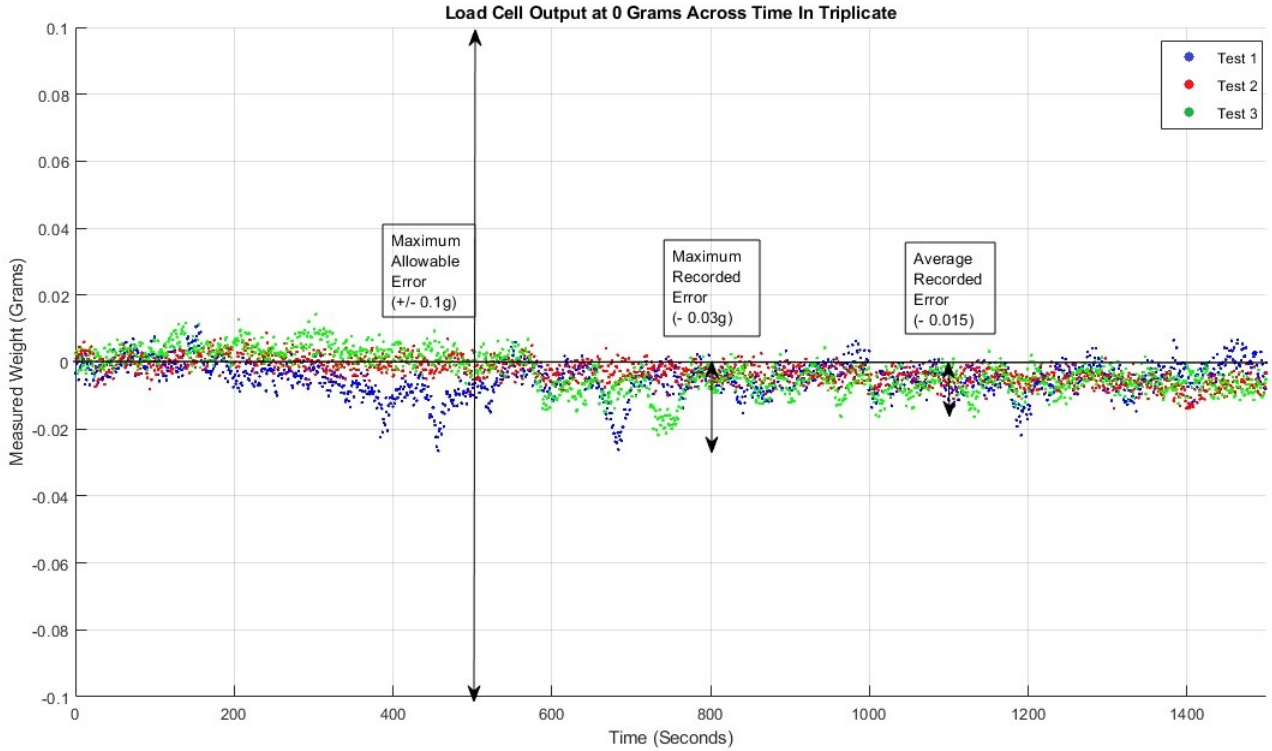


Figure 5.3: Graph of the digital output of the load cell when 0 grams is applied. The load cell output stabilizes around the true value of 0 grams without drifting outside of acceptable error over the course of time. The load cell output is also precise as the output between independent tests does not vary outside of acceptable bounds from each other.

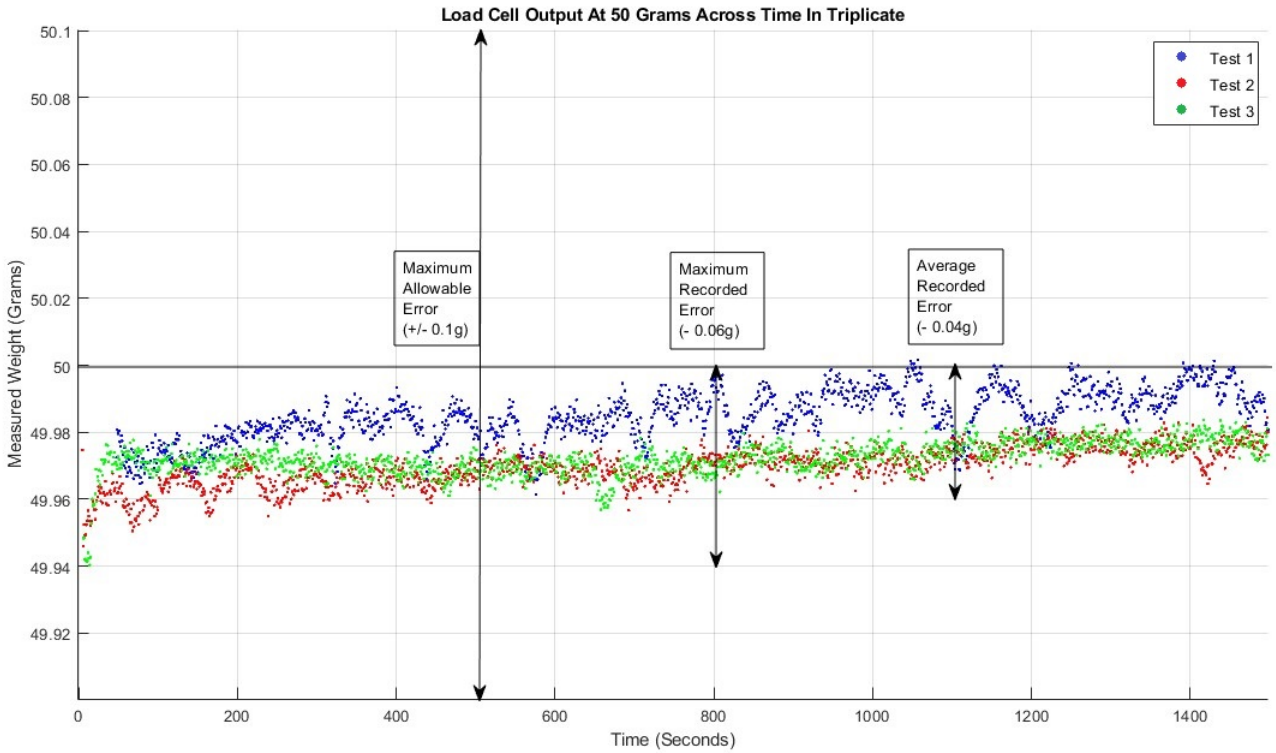


Figure 5.4: Graph of the digital output of the load cell when 50 grams is applied. The load cell output stabilizes around the true value of 50 grams without drifting outside of acceptable error over the course of time. The load cell output is also precise as the output between independent tests does not vary outside of acceptable bounds from each other.

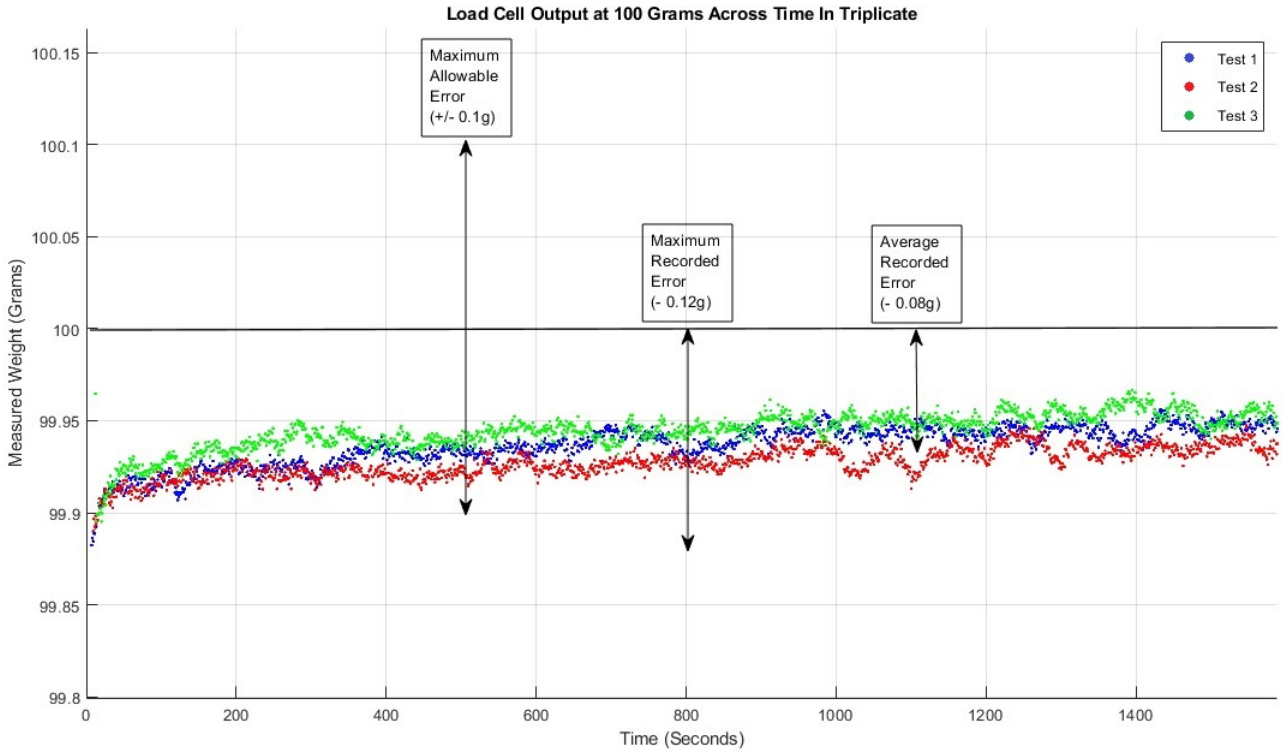


Figure 5.5: Graph of the digital output of the load cell when 100 grams is applied. The load cell output stabilizes around the true value of 100 grams within the acceptable error. However, initially the load cell reading is outside of acceptable error and take some significant amount of time to stabilize. The load cell output is also precise as the output between independent tests does not vary outside of acceptable bounds from each other.

From the accuracy test, the following conclusions were drawn. The low-end weight feedback system is capable of measuring masses across the 0 gram to 100 gram range with an accuracy of less than one decigram. Outside of the 0 gram to 100 gram range, the accuracy of the weight measurements is greater than one decigram.

From the precision test, the following conclusions were drawn. The low-end weight feedback system is capable of measuring masses across the 0 gram to 100 gram range with a precision of +/- fifteen milligrams. Outside of the 0 gram to 100 gram range, the precision of the weight measurement begins to show variances in the decigram range.

## 5.3 Pumping Element Design & Tests

### 5.3.1 Screw Cross Section Output Tests

The cross section shape and size of varying screws were experimentally investigated. A small cross section is desirable but unreliable. As the size of the cross section decreases, so does the rate of flow of powder through the cross section [3]. This allows for greater control over the delivered dose due to the decreased flow rate.

However, there is a critical point where the cross section becomes so small that the powder can not freely flow. This causes the flow rate to become unstable and thus the mechanism becomes unreliable. For this reason, powder flow tests were conducted on a variety of screws. A model of the apparatus used for conducting these tests can be seen in 5.6

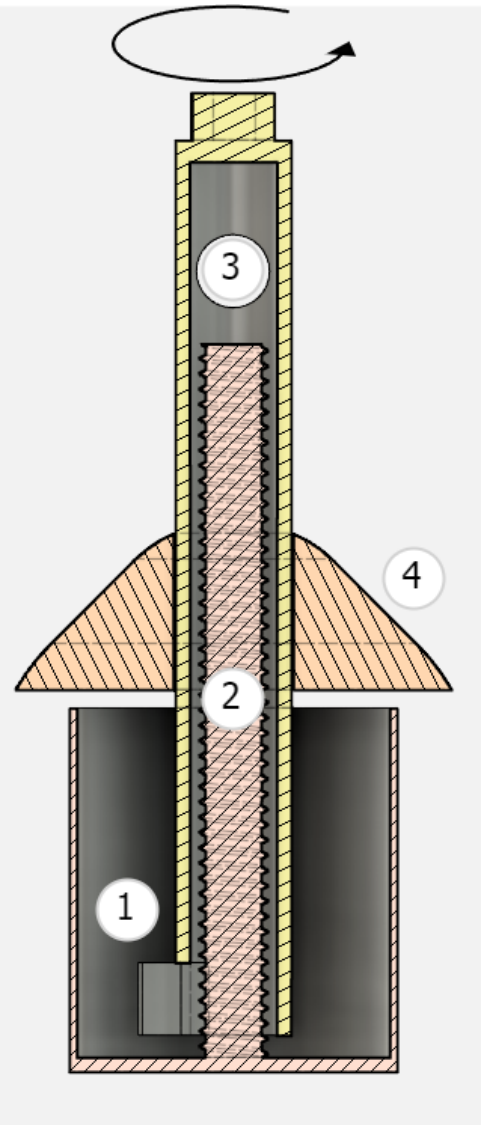


Figure 5.6: Apparatus used for measuring screw cross section and output rate. Powder is stored in (1). The housing in yellow rotates anticlockwise about a static screw in pink (2). This induces upwards flow of the powder from (1) to (3). Upon reaching (3), the centrifugal force of the rotating housing causes the powder to be ejected. The ejected powder is prevented from recirculating by the orange shielding cone (4). By preventing recirculation, the shielding cone (4) enables the use of loss-in-weight techniques to measure powder output. It should also be noted that the ejection port marked by (3) was seal with a plug of a known mass in order to avoid spillage before weighing.

| | No-Flow | Weak-Flow | Strong-Flow |
|---|---|---|---|
| Trapezoidal 8-TPI | | | X |
| Trapezoidal 10-TPI | | | X |
| Trapezoidal 12-TPI | | X | |
| Trapezoidal 16-TPI | | X | |
| Trapezoidal 20-TPI | X | | |

Table 5.1: Evaluation of 'ACME' trapezoidal threads with varying pitches.

The evaluation of the effect of screw cross section size on powder flowability was done visually. Screws cross sections evaluations fell into (3) distinct sets: No-Flow, Weak-Flow, and Strong-Flow. A screw that falls into the No-Flow set has little to no flow at the outlet. A screw that falls into the Weak-Flow set has flow at the outlet; but this flow is either unstable, insignificant, or both. A screw that falls into the Strong-Flow set has both stable and significant flow at the outlet.

With this information, it can be reasonably determined what the lower end of the range of cross sections sizes in which Weak-Flow transitions into Strong-Flow. Put simply, this information will help to determine a good cross section size for stable yet minimal flow. All screws evaluated had a major diameter of $\frac{3}{8}$ inches. The major variants between screws are (a) thread shape and (b) threads per inch, also known as the pitch.

| | No-Flow | Weak-Flow | Strong-Flow |
|---|---|---|---|
| Triangular 8-TPI | | X | |
| Triangular 10-TPI | | X | |
| Triangular 12-TPI | | X | |
| Triangular 16-TPI | X | | |
| Triangular 20-TPI | X | | |

Table 5.2: Evaluation of triangular 'Sharp V' threads with varying pitches.

| | No-Flow | Weak-Flow | Strong-Flow |
|---|---|---|---|
| Circular 8-TPI | | | X |
| Circular 10-TPI | | | X |
| Circular 12-TPI | | | X |
| Circular 16-TPI | | X | |
| Circular 20-TPI | | X | |

Table 5.3: Evaluation of circular 'Knuckle' threads with varying pitches.

From the evaluations in 5.1, 5.2, and 5.3; two major design conclusions were drawn. Firstly, triangular 'Sharp V' threads are a sub-optimal choice and circular 'Knuckle' threads are an optimal choice. Secondly, the range in which strong stable flow occurs for this particular sodium bicarbonate powder as a function of thread pitch is between 10 TPI and 16 TPI. Thus, when designing the pumping element, a trapezoidal or circular thread shape with 10 to 16 threads per inch is ideal.

Using the equation for the area of a circle 5.7 and the previously determined optimal threads per inch; the effective cross sectional area for strong powder flow can be determined.

$$A = \pi r^2 \tag{5.7}$$

Using the optimal TPI for a circular threads is between 10 and 16 TPI, it is determined that the optimal diameter is between $\frac{1}{10}$ and $\frac{1}{16}$ of an inch. Thus the optimal radii is between $\frac{1}{20}$ and $\frac{1}{32}$. Applying this information 5.7 allows us to determine that the optimal cross sectional area is between 0.003068 and 0.007854 $in^2$.

### 5.3.2 Pumping Element Design

A prototype of the pump was FDM 3D printed out of polyethylene terephthalate glycol (PETG). The pump is designed to operate at room temperature and ambient pressure. The pump is designed to be operated by an electric stepper motor which is wave driven. 5.7.

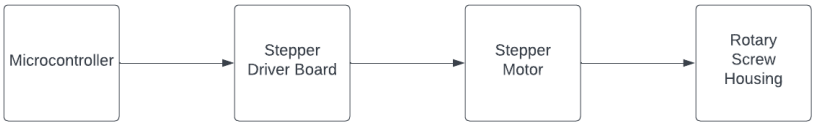


Figure 5.7: Open Loop Control Diagram of Pumping Element

An example of the pumping element can be seen in 5.8. Current work being done sees an offspring of this design being form fitted into an airtight, stainless steel hull. The static screw as well as the rotary screw housing are all fabricated from stainless steel and maintain tolerances within a few thousandths of an inch.

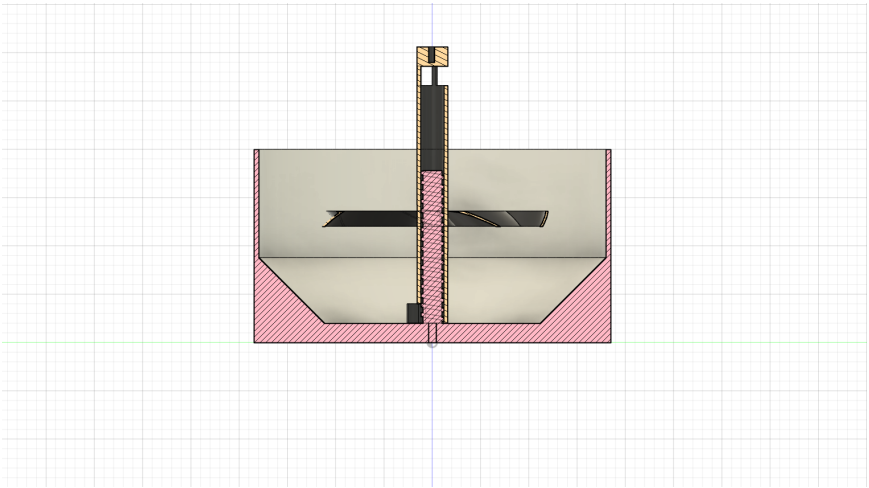

Figure 5.8: The primary internals of the pumping element. The external bulk housing and internal static screw can be seen in pink. Surrounding the internal screw is the rotary screw housing in yellow. Jutting out from the rotary screw housing in black is the toroidal impellor/agitator. The importance of the agitator cannot be over stressed. The agitator both breaks down force chains before they can fully propagate as well as assists in keeping the pump inlet saturated by shaping and directing powder flow.

Figure 5.9: A more explicit view of the toroidal agitator and the rotary screw housing that it is attached to.

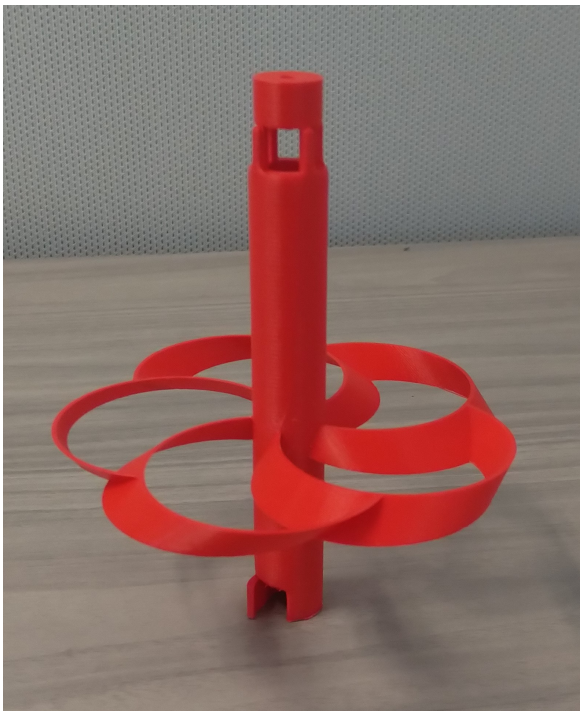

Figure 5.10: The fabricated toroidal agitator.

### 5.3.3 Pumping Element Tests

The pumping element as seen in 5.6 was experimentally tested for its rate of flow and its longevity. Due to the lack of a Hall Flow Meter, which can be used to measure flow in continuous time, tests were conducted using discrete amounts of time. Tests were done by driving the pumping element at a constant rate for a set amount of time and measuring the loss in weight.

The pumping element was driven at a rate of 250 revolutions per minute (RPM). The discrete time increment the pump was driven for is 10 seconds. After being driven for 10 seconds, the shielding cone was gently brushed clean and the loss

in weight of the testing apparatus 5.6 was determined. With the weight of powder dispensed per ten seconds known, an approximate flow rate can be calculated.

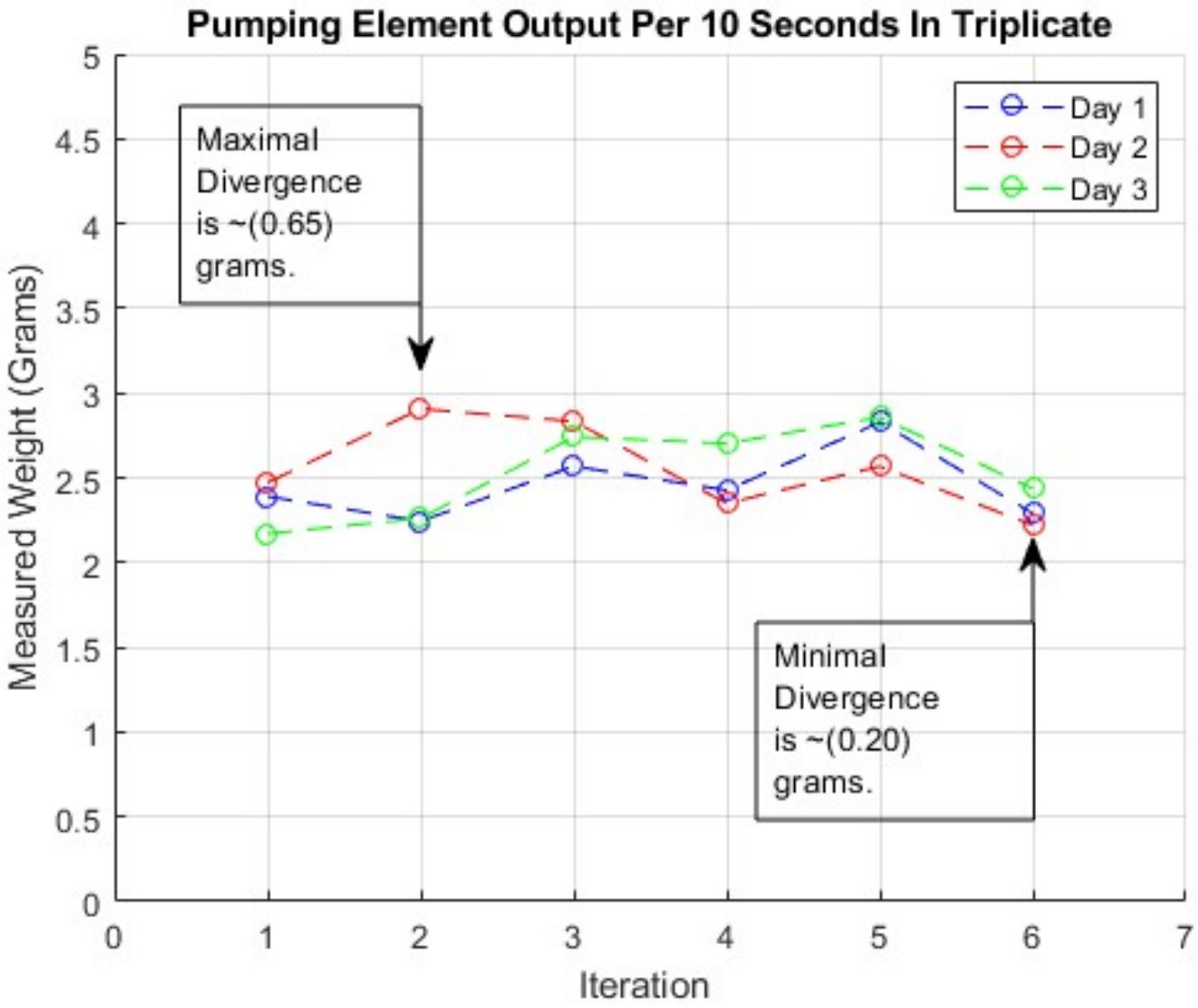


Figure 5.11: Pump output per 10 seconds. Note that between each separate day, the pump was configured to recirculate while running overnight. Then the battery of 10 seconds tests was run again. This was done to investigate the robustness of the system.

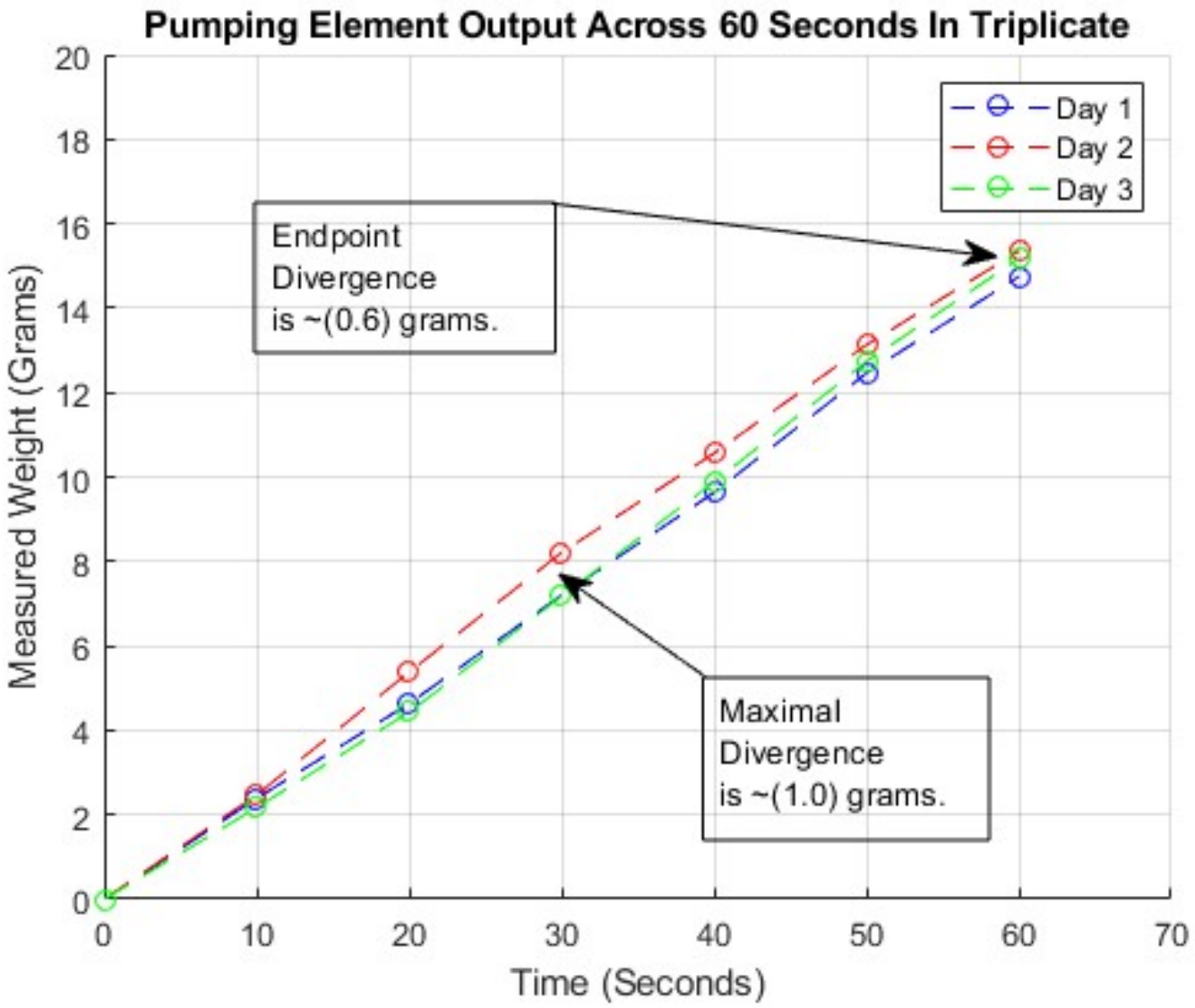


Figure 5.12: The summed output of all six 10-second tests. The accumulated variations across time support the notion that a closed loop system is needed for accurate dosing.

It should be noted that the amount of powder dispensed per revolution can also be calculated, allowing for a higher level of precision. The caveat of this is that the powder dispensed per revolution is a function of the RPM. Thus any calculations done for dispensation per revolution only hold true at a constant RPM.

## 5.4 Dispenser Body

### 5.4.1 Dispenser Body Design

The physical dispenser body has 5 main components. These can be seen in 5.13. These components were specifically designed with FDM 3D printing in mind. However, it would be possible to fabricate them out of a combination of stamped sheet metal and machined parts.

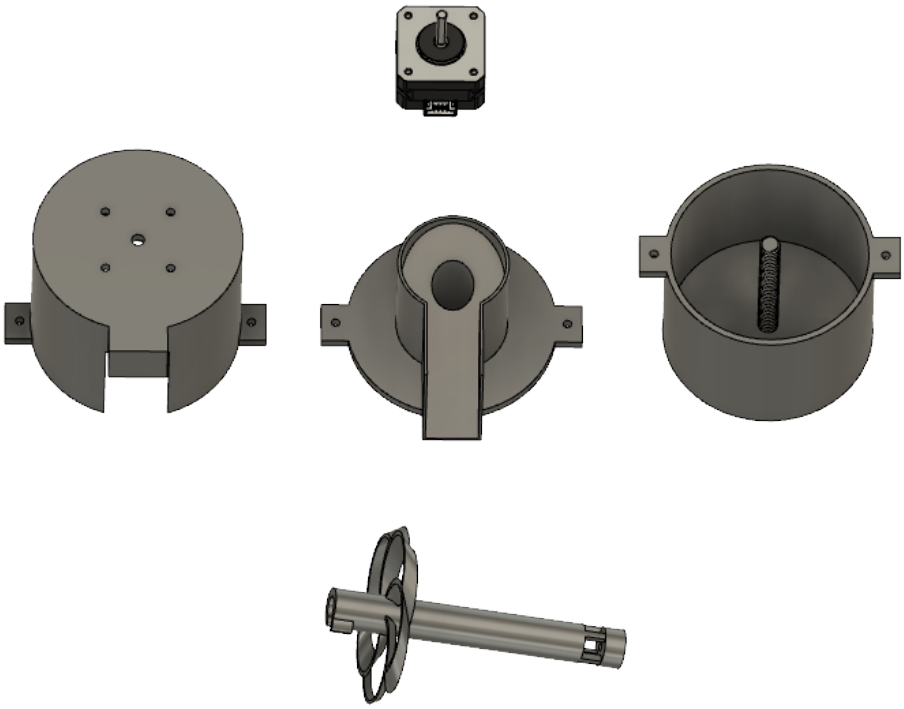

Figure 5.13: Models of the 5 main components of the prototype dispenser body. From top to bottom and left to right these components are: the drive stepper motor, the cover with motor mounting points, the feed slope and spray catcher, the tank housing with static feed screw, and the rotary pump housing with the attached toroidal agitator.

The full assembly of the 5 main components can be found in 5.14. The pieces are then kept together using the compressive force of (2) M4 nuts with bolts.

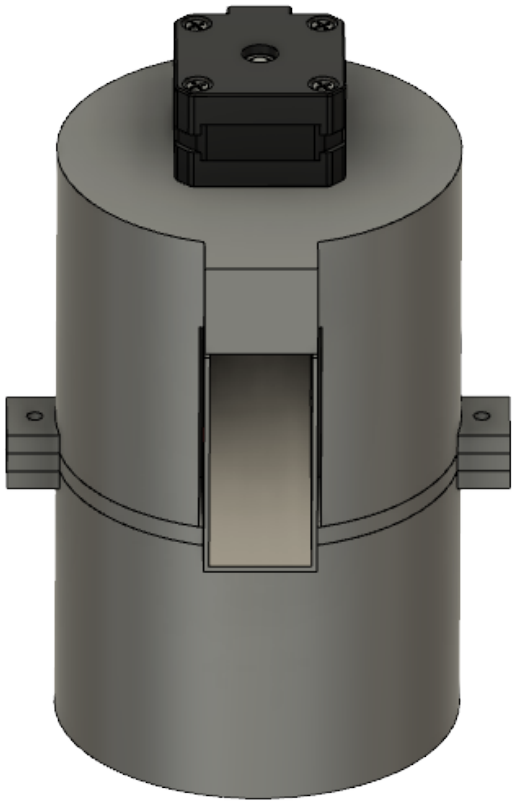

Figure 5.14: A model of the assembled prototype dispenser body.

A cross sectional side view of the dispenser body can be found in 5.15. Some important features to note are the implementation of the pumping element and toroidal agitator as seen in 5.6 and the feed slope with an angle of descent larger than the angle of repose.

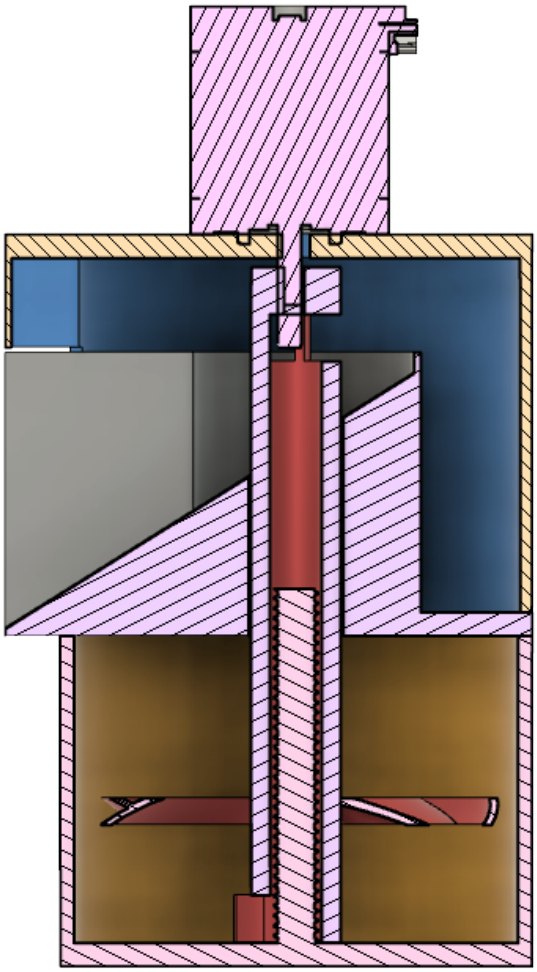

Figure 5.15: A cross section analysis of the prototype dispenser body.

### 5.4.2 Dispenser Body Fabrication

A prototype of the dispenser body was FDM 3D printed out of polyethylene terephthalate glycol 5.16 5.17. All components were printed with supports and required some post processing. Specifically, the feed slope requires wet sanding in order to bring down the surface roughness. Doing this helps to avoid stagnation of flow from the pumping element output through the feed slope.

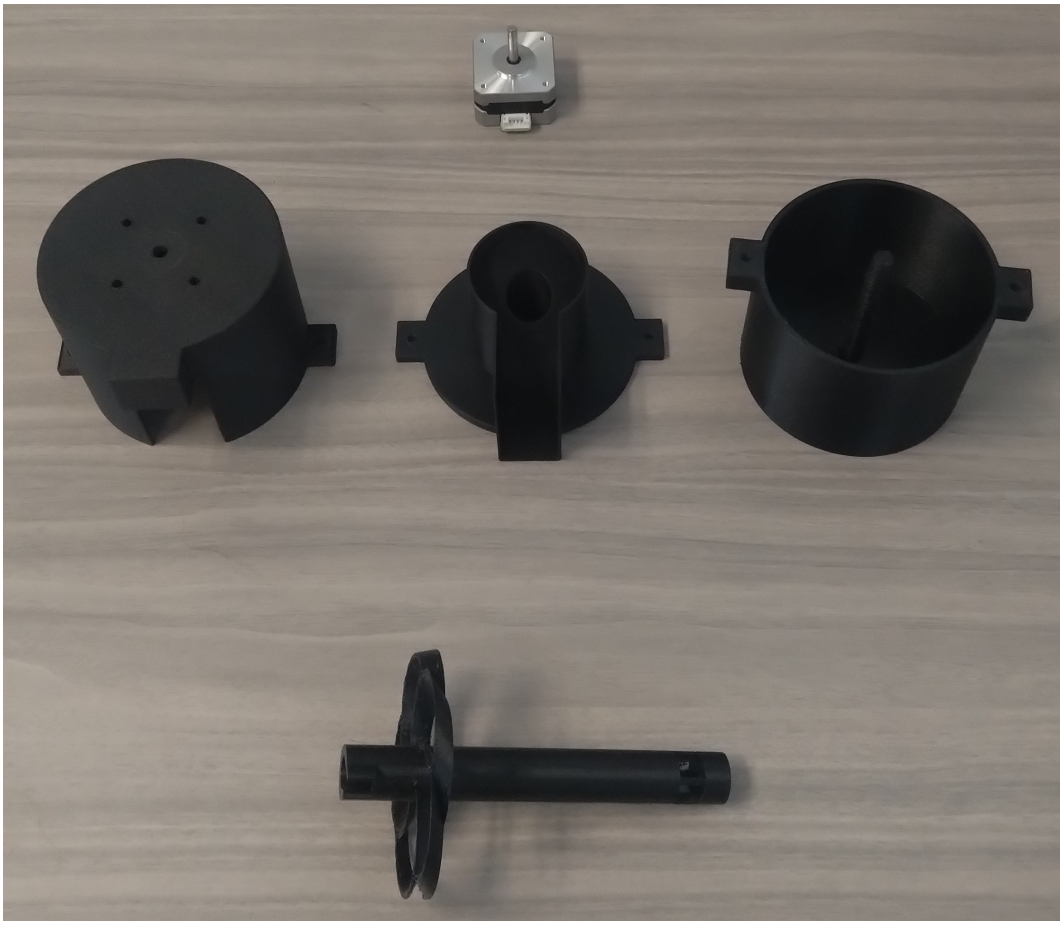

Figure 5.16: The 5 main components of the prototype dispenser body.

The 3D printed components that make up the dispenser body are help together by 2 M4 nuts and bolts. The stepper motor is mounted into the top by 4 M3 screws. The stepper motor drive shaft is fitted into the receiving end of the toroidal agitator.


Figure 5.17: The assembled prototype dispenser body.

# Chapter 6

# Future Work

Future work is currently underway, albeit rather slowly. The accuracy of the weight feedback system leaves much to be desired. Greater dominion over the relationship between the pumping element and the weight feedback system through PID control is also desired. In regards to the pumping element, it is currently too big in size and lacks durability due to the plastic materials used in its construction. Let us briefly consider some of these issues.

## 6.1 High-End Weight Feedback System

### 6.1.1 Dispensation To Target

Currently the dispenser body is able to dose out powder onto the mass feedback element. However there currently is no mechanism to move the powder from the mass feedback element to the target location. Currently, two possible options are being

investigated.

The first option is to design, fabricate, and validate a mechanism to rotate the mass feedback element so that the powder falls into the target under the force of gravity. The second option is to mount the mass feedback element at an angle, so the powder continuously flows over it. Then, the signal from the mass feedback element could be integrated over time in order to track the overall mass. Of the two options, the former seems more reliable in terms of accuracy and precision.

### 6.1.2 Milligram Accuracy

The low-end weight feedback system meets the specifications set within our objectives. But it could be better. Future works hopes to see the implementation of a high-end weight feedback system similar to that seen in [6]. Such a system can reliably measure dosages with milligram accuracy. Pursuing such a system within the confines of this thesis would violate one of the specifications stated within the Objective section. This is due to the price associated with the high-end weight feedback system.

### 6.1.3 PID Control

The pumping element and load cell, in their current state, are operated by a 'Bang-Bang' controller[1]. The accuracy of the dosage could be vastly improved with PID control. Similarly, the amount of time needed to dispense and measure a dose could be vastly improved with PID control. One possible solution to this issue can be seen below

[1] A 'Bang-Bang' controller is a controller that operates between two states: On and Off.

in 6.1.

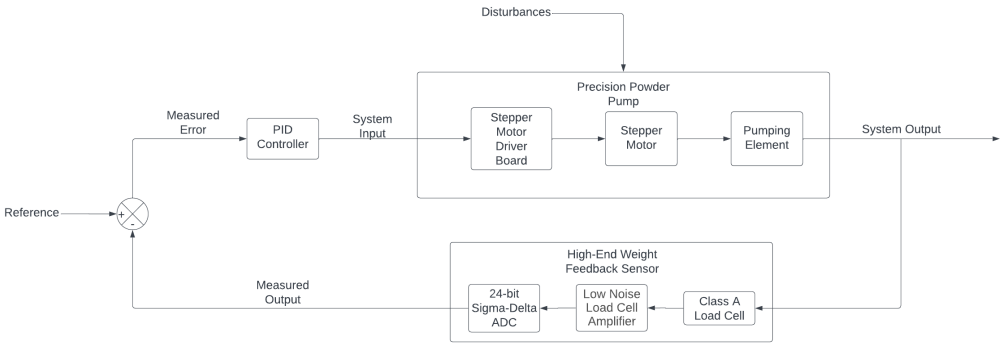


Figure 6.1: System diagram of proposed implementation of PID control.

## 6.2 Revised Pumping Element

The pumping element design is currently undergoing revision. This revision can be broken into two distinct parts. The first part is to construct the pumping element out of stainless steel. The second part is to make the entire pumping element smaller. Let us briefly take a look at why these changes should be made.

### 6.2.1 Reduced Surface Roughness

The pumping element should be constructed out of stainless steel. Firstly, as powder flows through the pumping element, it will abrade the surface. If the pumping element is constantly being abraded by the flowing of powder, it will slowly but surely begin to lose precision. Stainless steel would decrease the amount of wear on the pumping element caused by this abrasion over the course of time.

### 6.2.2 More Compact Pumping Element

The pumping element could be significantly smaller. Making the pumping element smaller would allow for decreased feed rates and less costly construction. Decreased feed rates would allow us to approach that milligram level accuracy that we crave so very much. Less costly construction would allow for the system to be ran in parallel with copies of itself; thus leading to increased throughput. For industrial applications, this is a must.

# Chapter 7

# Conclusion

It has been shown that with the low-end weight feedback system, a measurement accuracy of +/- 15 milligrams is achievable. This was done at a total cost of about 30 USD. The caveat of the low-end weight feedback system is the few seconds of settling time required to make an accurate measurement. The accuracy of the system meets the specifications set within the objectives section. Decigram accuracy is achieved with a margin of safety of about 6. However, the accuracy could be much better. Milligram accuracy is achievable but not without violating the cost effectiveness stipulation.

In regards to the pumping element, the results 5.12 5.11 indicate that an open loop system cannot achieve the accuracy necessary. The pumping element shows stable output behavior. Additionally, the pumping element passed initial longevity tests. With this being said, the pumping element should still be revised. The pumping element should be fabricated out of stainless steel to a higher degree of precision. If the pumping element is revised, then the battery of tests should be revised as well.

# Bibliography

[1] Hamzah M. Beakawi Al-Hashemi and Omar S. Baghabra Al-Amoudi. A review on the angle of repose of granular materials. 330:397–417.

[2] M. O. Besenhard, S. Fathollahi, E. Siegmann, E. Slama, E. Faulhammer, and J. G. Khinast. Micro-feeding and dosing of powders via a small-scale powder pump. 519(1):314–322.

[3] M. O. Besenhard, S. K. Karkala, E. Faulhammer, S. Fathollahi, R. Ramachandran, and J. G. Khinast. Continuous feeding of low-dose APIs via periodic micro dosing. 509(1):123–134.

[4] Christopher E Brennen. *Internal flow energy conversion*. Cambridge University Press, Cambridge, April 2005.

[5] CE Davies, SJ Tallon, and N Brown. Continuous monitoring of bulk density and particle size in flowable powders and grains. *Chemical Engineering Research and Design*, 83(7):782–787, 2005.

[6] Analog Devices. Precision weigh scale design using the ad7191 24-bit sigma-delta adc with internal pga.

[7] Sara Fathollahi, Stephan Sacher, M. Sebastian Escotet-Espinoza, James DiNunzio, and Johannes G. Khinast. Performance evaluation of a high-precision low-dose powder feeder. 21(8):301.

[8] V. Garg, T. Deng, and M.S.A. Bradley. A new method for assessing powder flowability based on physical properties and cohesiveness of particles using a small quantity of samples. 395:708–19. Place: Netherlands Publisher: Elsevier B.V.

[9] G. R. Higson. Recent advances in strain gauges. 41(7):405.

[10] Jin-Yuan Lin, Jing-Min Lin, Chin-Chuan Han, Yu-Chi Wu, and Chao-Shu Chang. An automatic chinese medicine dispensing machine using shelf-based mechanism. 9(23):5060. Number: 23 Publisher: Multidisciplinary Digital Publishing Institute.

[11] A Sanket Hiralal Lunawat and Kiran C More. Design and analysis of bucket elavator. *Asian Journal For Convergence In Technology (AJCT) ISSN-2350-1146*, 4(3), 2018.

[12] Shuji Matsusaka, Koji Yamamoto, and Hiroaki Masuda. Micro-feeding of a fine powder using a vibrating capillary tube. 7(2):141–151.

[13] W. McBride and P. W. Cleary. An investigation and optimization of the 'OLDS' elevator using discrete element modeling. 193(3):216–234.

[14] F J_ C Rademacher. Non-spill discharge characteristics of bucket elevators. *Powder Technology*, 22(2):215–241, 1979.

[15] Alan W Roberts. The influence of granular vortex motion on the volumetric performance of enclosed screw conveyors. *Powder Technology*, 104(1):56–67, 1999.

[16] Yohei Maurice Rosen. *Tools for large and detailed experiments in genomics and tissue development.* phdthesis.

[17] Stephan Sacher, Sara Fathollahi, and Johannes G. Khinast. Comparative study of a novel micro-feeder and loss-in-weight feeders. 17(4):1205–1214.

[18] Ravendra Singh, Andrés D Román-Ospino, Rodolfo J Romañach, Marianthi Ierapetritou, and Rohit Ramachandran. Real time monitoring of powder blend bulk density for coupled feed-forward/feed-back control of a continuous direct compaction tablet manufacturing process. *International journal of pharmaceutics*, 495(1):612–625, 2015.

[19] IC Sinka, SF Burch, JH Tweed, and JC Cunningham. Measurement of density variations in tablets using x-ray computed tomography. *International Journal of Pharmaceutics*, 271(1-2):215–224, 2004.

[20] John A Slotwinski, Edward J Garboczi, and Keith M Hebenstreit. Porosity measurements and analysis for metal additive manufacturing process control. *Journal of research of the National Institute of Standards and Technology*, 119:494, 2014.

[21] Hongyuan Sun, Huaqing Ma, and Yongzhi Zhao. DEM investigation on conveying of non-spherical particles in a screw conveyor. 65:17–31.

[22] Samir Trabelsi, Ana M Paz, and Stuart O Nelson. Microwave dielectric method for the rapid, non-destructive determination of bulk density and moisture content of peanut hull pellets. *Biosystems engineering*, 115(3):332–338, 2013.

[23] Chunbao Xu and Jesse Zhu. Parametric study of fine particle fluidization under mechanical vibration. 161(2):135–144.

[24] Wenbiao Zhang, Chao Wang, Wuqiang Yang, and Chi-Hwa Wang. Application of electrical capacitance tomography in particulate process measurement–a review. *Advanced Powder Technology*, 25(1):174–188, 2014.